Heliyon 6 (2020) e03251

Contents lists available at ScienceDirect

Heliyon

journal homepage: www.cell.com/heliyon

Research article

Tracking changes of the parameters of glucose-insulin homeostasis during the course of obesity in B6D2F1 mice

Sakineh Esmaeili Mohsen Abadi [a], Ramin Balouchzadeh [a], Guney Uzun [a], Hoo Sang Ko [a], H. Felix Lee [a], Sarah Park [c], Guim Kwon [b,*]

[a] School of Engineering, Southern Illinois University Edwardsville, Edwardsville, IL, 62026, United States
[b] School of Pharmacy, Southern Illinois University Edwardsville, Edwardsville, IL, 62026, United States
[c] Library and Information Services, Southern Illinois University Edwardsville, Edwardsville, IL, 62026, United States

ARTICLE INFO

Keywords:
Biochemistry
Glucose-insulin homeostasis
Type 2 diabetes
Insulin
Obesity
High fat diet
Mathematical modeling
Rate constants

ABSTRACT

Obesity is one of the primary causes of type 2 diabetes mellitus (T2DM). To better understand how obesity impairs glucose-insulin homeostasis, we tracked fasting blood glucose and insulin levels and the key components of glucose-insulin homeostasis for 7 months in high fat diet (HFD; 45% fat) fed mice (n = 8). Every 2 weeks we measured body weight, fasting blood glucose and insulin levels, and estimated 5 key rate constants of glucose-insulin homeostasis using the methods established previously (Heliyon 3: e00310, 2017). Mice gained weight steadily, more than doubling their weights after 7 months (23.6 ± 0.5 to 52.3 ± 1.4 g). Fasting (basal) insulin levels were elevated (221.3 ± 16.7 to 1043.1 ± 90.5 pmol l^{-1}) but fasting blood glucose levels unexpectedly returned to the baseline levels (152.8 ± 7.0 to 152.0 ± 7.2 mg/dl) despite significantly elevated levels (216.8 ± 44.9 mg/dl, average of 3 highest values for 8 mice) during the experimental period. After 7 months of HFD feeding, the rate constants for insulin secretion (k_1), insulin-independent glucose uptake (k_3), and insulin concentration where liver switches from glucose uptake to release (I_{pi}) were significantly elevated. Insulin-dependent glucose uptake (k_2) and rate constant of liver glucose transfer (k_4) were lowered but no statistical significance was reached. The novel and key finding of this study is the wide range of fluctuations of the rate constants during the course of obesity, reflecting the body's compensatory responses against metabolic alterations caused by obesity.

1. Introduction

Type 2 diabetes mellitus (T2DM), the most prevalent form of diabetes, affects ~380 million people around the world (2014 statistics, World Health Organization). The causes of T2DM include a mixture of genetic predisposition and environmental factors. Among these, obesity is one of the primary risk factors that cause T2DM. Obesity, especially visceral fat accumulation, is known to cause systemic insulin resistance, elevating blood glucose levels in the body [1, 2, 3]. Adequate compensatory responses of pancreatic β-cells through hypersecretion of insulin, however, is thought to protect an obese individual from developing T2DM [4, 5]. Genetic predisposition may affect an individual to be more susceptible to insulin resistance and/or β-cell failure in the setting of obesity [6]. Thus, not all obese individuals develop T2DM.

Extensive research has elucidated the link between obesity and T2DM, which involves proinflammatory cytokines (tumor necrosis factor and interleukin-6), insulin resistance, glucolipotoxicity associated with nutrient overload, and alterations in cellular processes such as mitochondrial dysfunction and endoplasmic reticulum stress in β-cells and other tissues [7, 8, 9, 10]. However, comprehensive understanding of how the physiology of the body changes during the course of obesity is lacking. For example, it is well documented that insulin secretion from pancreatic β-cells increases initially to compensate insulin resistance in the peripheral tissues but decreases over time due to β-cell dysfunction and destruction [11, 12]. It is not known, however, how the process of the changes occurs whether it is a gradual and linear, stepwise, or any other pattern. It is also not known if other parameters of glucose-insulin homeostasis that affect muscle, liver, and adipocytes also fluctuate similar to insulin secretion.

Despite theoretical and technical limitations, several models including homeostatic model assessment (HOMA), intravenous and oral glucose tolerance tests (IVGTT and OGTT), calculation of insulin/C-peptide ratio, and hyperglycemic clamp have been developed to assess *in vivo* β-cell function for clinical and research purposes. Among these

* Corresponding author.
E-mail address: gkwon@siue.edu (G. Kwon).

https://doi.org/10.1016/j.heliyon.2020.e03251
Received 26 June 2019; Received in revised form 25 October 2019; Accepted 14 January 2020

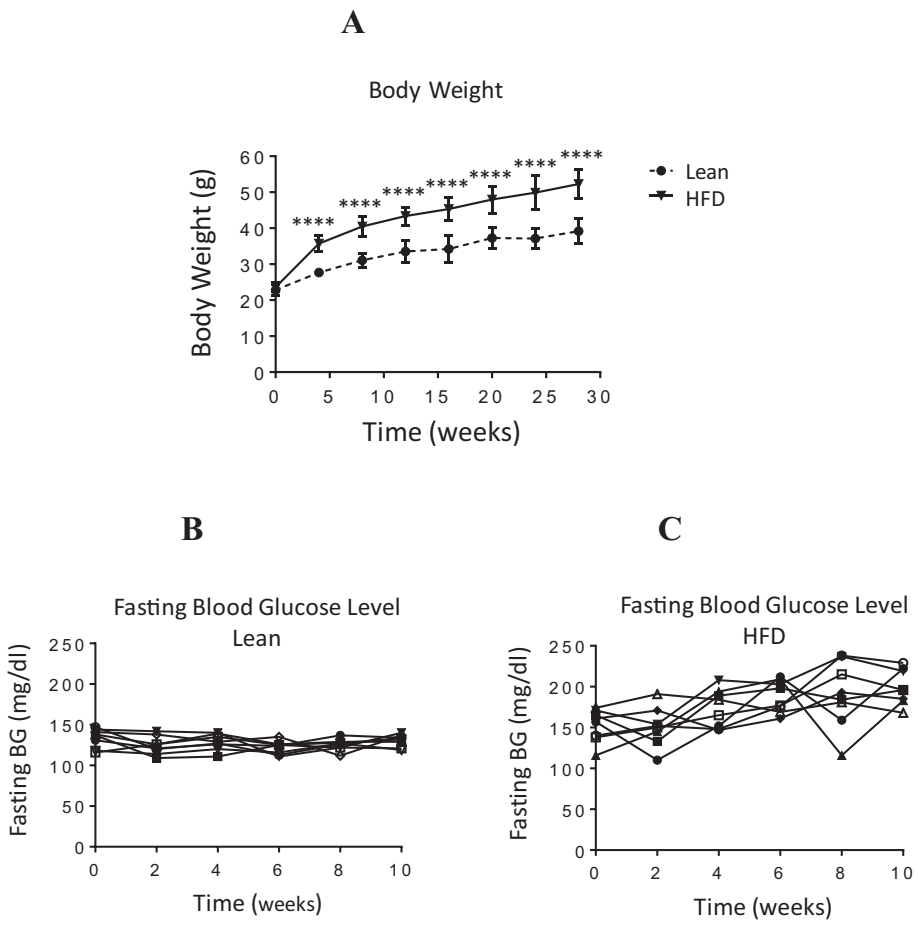

Figure 1. (A) Body weights of mice (n = 8) fed with lean diet or HFD over 28 weeks. (B) and (C) Fasting blood glucose levels of lean diet- and HFD-fed mice, respectively. Mice were fasted for 5 h and blood glucose levels were determined using Contour glucose meter collecting blood from the tip of the tail.

methods, hyperglycemic clamp [13] is considered as 'gold standard' with highly reproducible and reliable assessment of β-cell responsivity to glucose. However, technical difficulties requiring highly specialized expertise limit its wide usage in regular laboratories. Moreover, methods for *in vivo* assessment of various other parameters that determine glucose-insulin homeostasis in tissues such as muscle, liver, and other tissues are difficult and usage of radioactive materials is necessary [14]. In animals, termination of life is often required to perform biochemical, biophysical, and molecular biology experiments on specific tissues to assess these. To track the alterations in the parameters of glucose-insulin homeostasis non-invasively in live animals, we have previously established methodologies for estimating insulin secretion, glucose uptake by tissues, and liver handling of glucose using a modified mathematical model of Lombarte et al. [15].

The primary objective of this study was to see if there exists a threshold, a distinct time point when a path to diabetes is committed during the course of obesity due to significant pathophysiologic alterations in various organs. Display of continuously sustained high fasting blood glucose levels with severe systemic insulin resistance beyond a time point would have been confirmatory to existence of such a threshold. To this end, we tracked the changes of fasting blood glucose, basal insulin, and various parameters of glucose-insulin homeostasis for 7 months in HFD-fed mice. Contrary to our hypothesis, we have not observed such a threshold that displays concerted changes of the parameters to a path to diabetes. Despite doubling of the body weight, fasting blood glucose levels returned to the baseline levels after 7 months of HFD feeding. Unexpectedly, we have also found that virtually all the parameters showed a wide range of fluctuations during the course of obesity. Especially, insulin-independent glucose uptake (k_3) and blood insulin concentrations that regulate liver switch of glucose uptake and release (I_{pi}) showed the most significant and dynamic changes. It is noteworthy that similar to insulin secretion (k_1) insulin sensitivity of the tissues (k_2) and the hepatic sensitivity to insulin (k_4) were also elevated during the course of obesity, suggesting that compensatory responses may occur not only in pancreatic β-cells but also in insulin-sensitive tissues. This is a novel and new concept that has not been explored previously. Establishing a methodology that provides comprehensive understanding of the physiology at different stages of the pathogenesis of obesity-mediated T2DM would provide valuable insights for designing strategies to prevent and/or delay the progression of the disease.

2. Materials and methods

2.1. Animals

Male B6D2F1 mice (the F1 hybrids of C57BL/6 and DBA/2, 4–6 weeks) were purchased from Harlan Sprague-Dawley Inc. (Indianapolis, IN) and were maintained in the animal facility at the School of pharmacy at Southern Illinois University Edwardsville (SIUE) under controlled conditions (temperature 68–73 °F and 12 h light-dark cycle). We chose to use male B62DF1 mice because these mice fed a high fat diet have been shown to develop diabetic symptoms characterized by hyperglycemia, glucosuria, and elevated hemoglobin A1C levels [16], whereas female mice were resistant to weight gain and showed no metabolic alterations

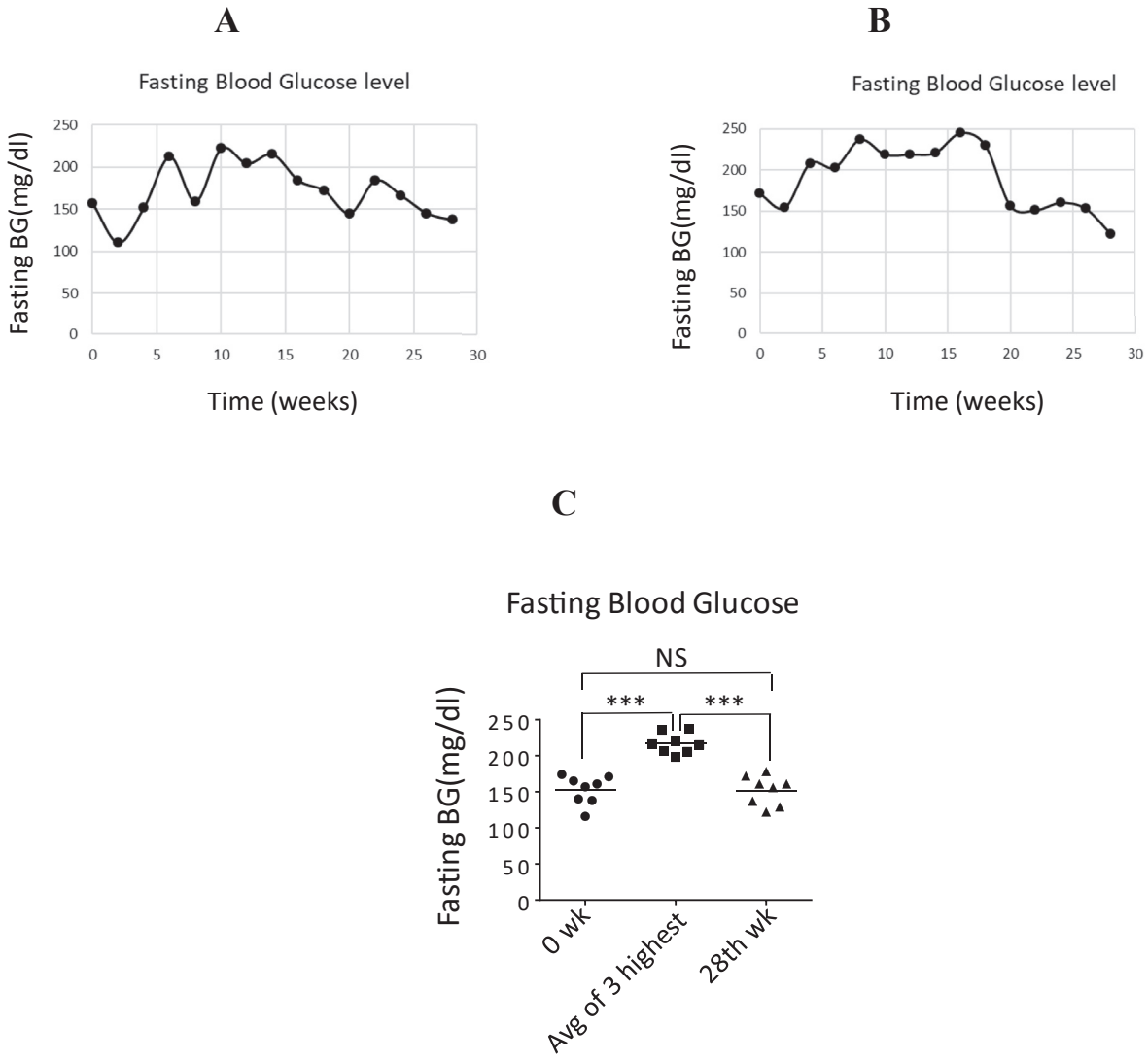

Figure 2. (A) and (B) Changes of fasting blood glucose levels of two representative mice over 28 weeks. (C) Mean fasting blood glucose levels (n = 8) at start (wk 0), during (average of 3 highest values), and end (wk 28) are shown.

Table 1. Summary of the data showing metabolic changes due to HFD feeding. Changes of body weights, fasting blood glucose and insulin levels as well as 5 rate constants that determine glucose-insulin homeostasis at start (wk 0), during (average of 3 highest values), and end (wk 28) are shown. Values are presented as mean ± SEM (n = 8). 'a' and 'b' denote significant differences between start vs. during and during vs. end, respectively. 'c' denotes significant differences between start (wk 0) and end (wk 28). NS denotes no significant difference between the groups.

	Start (wk 0)	Avg of 3 highest	End (wk 28)
Body weight (g)	23.6 ± 0.5		52.3 ± 1.4^{c}
Fasting BG (mg dl^{-1})	152.8 ± 7.0	$2l6.8 \pm 4.9^{a,b}$	152.0 ± 7.2^{NS}
Basal insulin ($pmol^{-1}$)	221.3 ± 16.7	$1365.9 \pm 110.6^{a,b}$	1043.1 ± 90.5^{c}
I_{pi} ($pmol^{-1}$)	491.0 ± 111.8	$2118.5 \pm l29.4^{a,b}$	963.3 ± 164.2^{c}
K_1 (pmol dl min^{-1} $mg^{-1}/^{-1}$)	0.23 ± 0.03	$1.92 \pm 0.16^{a,NS}$	1.47 ± 0.22^{c}
K_2 (mg/dl^{-1} min $pmol^{-1}$)	0.19 ± 0.04	$0.47 \pm 0.06^{a,b}$	0.07 ± 0.03^{NS}
K_3 (mg dl^{-1} min^{-1})	1.82 ± 0.67	$9.35 \pm 0.19^{a,NS}$	5.47 ± 1.46^{c}
K_4 (mg/dl^{-1} min $pmol^{-1}$)	0.11 ± 0.06	$0.44 \pm 0.08^{a,b}$	$0.0810.01^{NS}$

when they were fed a HFD (unpublished observations). After a 2 week acclimation period, the mice (4 per cage) were fed a lean diet (El-Mel, St. Louis, MO) or a high fat diet (HFD, 45% kcal fat, Harlan laboratories, Madison, WI) and water *ad libitum*. Gross energy for lean diet (protein; 29.8%, carbohydrate; 56.7%, Fat; 13.4% by weight) and HFD (protein; 17.3%, carbohydrate; 47.6%, Fat; 23.2% by weight) are 4.09 kcal/g and 4.7 kcal/g, respectively. Every 2 weeks for 7 months body weights and fasting blood glucose levels were determined, followed by intraperitoneal glucose tolerance test (IPGTT) of which data were used to estimate 5 rate constants that determine glucose-insulin homeostasis. All animal maintenance and treatment protocols complied with the Guide for Care and Use of Laboratory Animals as adopted by the National Institute of Health and approved by the SIUE Institutional Animal Care and Use Committee (IACUC).

2.2. Determination of fasting blood glucose and insulin levels and intraperitoneal glucose tolerance test

To reduce the impact of the circadian rhythm and hormones such as cortisol and growth factors, experiments were performed on every other Tuesday afternoon at the same time. Mice were fasted for 5 h and blood (70 μl) was collected from the tip of the tail of each mouse using a Fisher brand heparinized capillary tube to measure basal insulin level. The mice were fasted for 5 h instead of overnight to minimize discomfort and because 1) overnight fasting provokes a catabolic state in mice and alters metabolic state [17,18], 2) hepatic glucose production was not

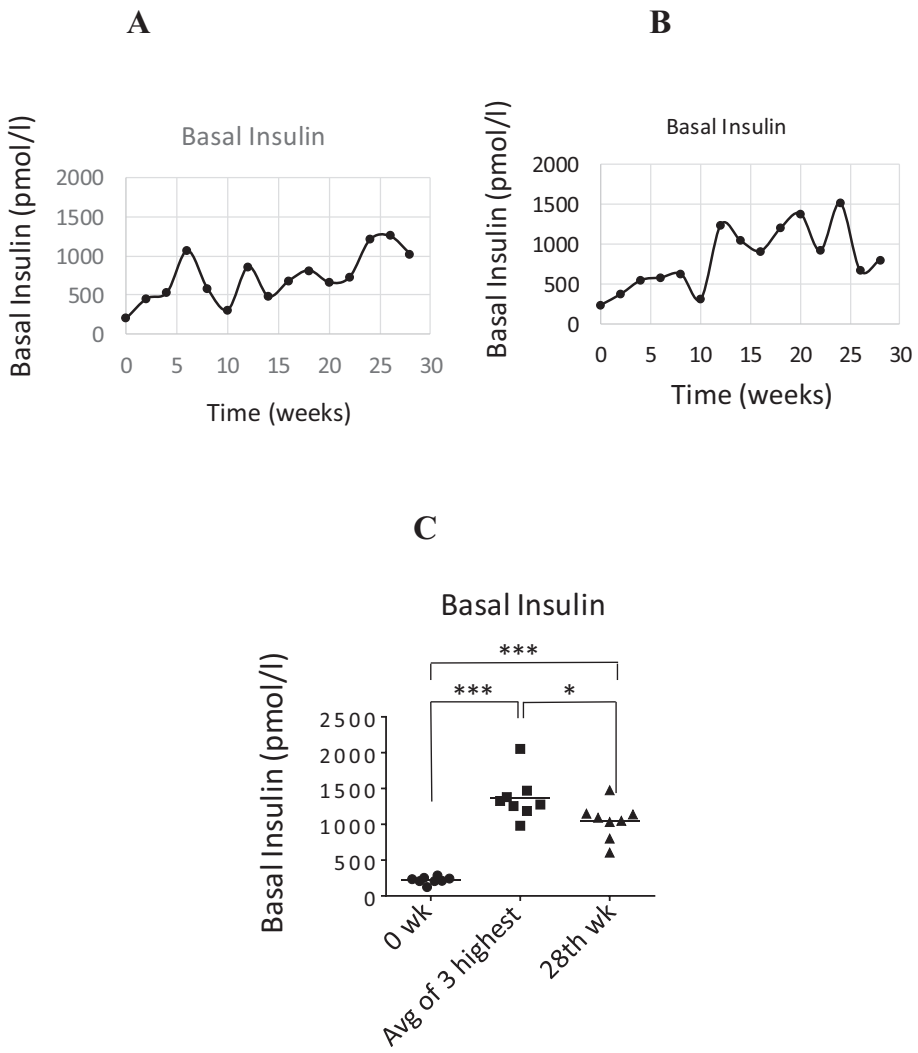

Figure 3. (A) and (B) Changes of fasting insulin levels of two representative mice over 28 weeks. (C) Mean fasting insulin levels (n = 8) at start (wk 0), during (average of 3 highest values), and end (wk 28) are shown.

significantly different from 4 to 16 h of fasting [17], and 3) there was no significant differences in the gastric content weight between 6 and 18 h fasted mice [19]. A 1:10 dilution of plasma was assayed for insulin content by radioimmunoassay (RIA) kit (Millipore) following the manufacturer's instructions. Basal insulin levels of the mice were determined every 2 weeks for 28 weeks. Mice were administered with 1 g/kg glucose by intraperitoneal injection using sterile 27G disposable needles. Blood glucose levels were determined using Contour glucose meter collecting blood from the tip of the tail at 0 (prior to glucose injection) and every minute for the first 16 min, every 2 min for the next 14 min, every 5 min until 1 h, and then every 15 min until 2 h. The frequency of blood glucose measurement was determined based on our previous studies that showed the peak occurs between ~15–30 min after glucose injection, followed by steady declining to basal or above basal levels. Frequent glucose measurement every 1 or 2 min during the first 30 min allowed us to capture the deflection of the blood glucose peak accurately.

2.3. Quantitation of β-cell area

Freshly isolated pancreases were placed in microfuge tubes, snap-frozen in liquid nitrogen, and stored at −70 °C until use. Every 10^{th} section of 10 μm thickness was collected and fixed in 4% paraformaldehyde and 1% Triton-X 100 in PBS. Pancreas sections were washed, blocked for 20 min in 2% BSA in PBS, and incubated for 30 min each with primary and secondary antibodies, insulin rabbit mAb and biotinylated secondary antibody, respectively. Following the manufacturer's instructions, tissues were stained with AB enzyme reagent, followed by peroxidase substrate containing DAB chromagen. Tissues were counterstained with Gill's formulation #2 hematoxylin and mounted on microscope slides. Images of pancreas sections were captured using a 2.5X objective in a Leica DMI inverted fluorescent microscope. The ratio of β-cell area to exocrine tissue area per section was calculated using the ImageJ image processing and analysis program.

2.4. Mathematical model

We used the mathematical model of glucose-insulin homeostasis proposed by Lombarte et al. [15] to study the extent to which the parameters of glucose-insulin homeostasis alter during the 7 months of HFD feeding. The proposed model consists of three differential equations that describe the changes of blood glucose (G), blood insulin (I), and the amount of glucose (D) in the peritoneal cavity over time.

$$dG/dt = -k_4(I - I_{pi}) - k_2I - k_3 + k_0D \quad (1)$$

$$dI/dt = k_1G - k_6I \quad (2)$$

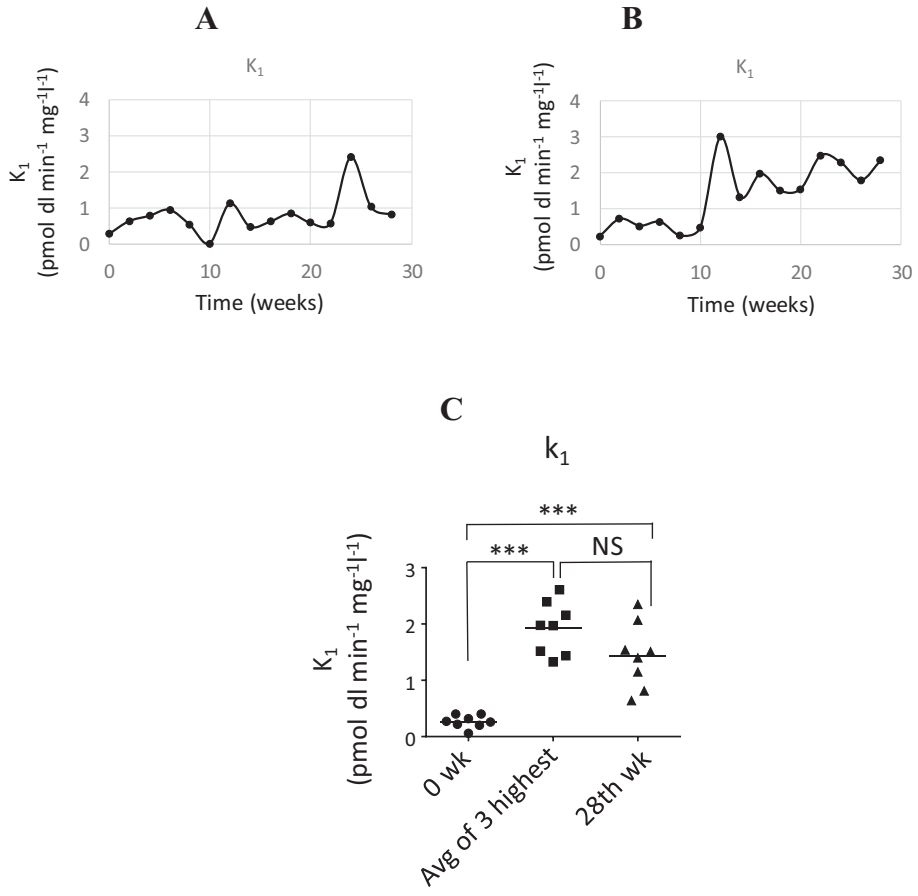

Figure 4. (A) and (B) Changes of the rate constant (k_1) of insulin secretion of two representative mice over 28 weeks. (C) Mean values of k_1 (n = 8) at start (wk 0), during (average of 3 highest values), and end (wk 28) are shown.

$$dD/dt = -k_aD \quad (3)$$

Brief descriptions of various parameters and terms in the three equations are summarized below. More detailed mathematical analysis and parameter estimation and validation can be found in the articles [15, 20]. Eq. (1) represents the change of blood glucose concentration over time. The term $k_4(I - I_{pi})$ represents the hepatic handling of glucose. I represents blood insulin concentration, I_{pi} represents blood insulin concentration when the liver changes from uptake to release of glucose, and k_4 is the rate constant of glucose transport in the liver. The k_2I term represents the insulin-dependent glucose uptake by the tissues including muscle, adipocytes, and liver. The k_3 term represents the insulin-independent glucose uptake by the tissues such as neuronal cells and white blood cells [21, 22]. The k_0D term represents the change in blood glucose concentration due to the intra-peritoneal injection of glucose.

Eq. (2) represents the change of blood insulin concentration over time. The term k_1G represents the pancreatic insulin secretion. The k_6I term represents blood insulin clearance.

Eq. (3) represents the change of glucose in the peritoneal cavity. The term K_a represents rate constant of glucose leaving the peritoneal cavity.

2.5. Simulation and optimization of the rate constants

We used Arena™ simulation (a program by Rockwell Software) combined with the OptQuest™ toolset to evaluate the mathematical model and optimally estimate the parameters. We developed a simulation program that incorporated the observed values in our experiments, the amount of glucose injected and initial parameter values as the simulation inputs. Using the inputs, the program created a continuous prediction of both insulin and glucose levels. The search algorithm of OptQuest™ evaluated various combinations of the parameters and determined the best set that minimized the sum of squared errors between the observed and the simulated data. Out of 8 parameters, we fixed three parameters including the rate constant of glucose entering blood from peritoneal cavity (k_0), the rate constant of insulin clearance from blood (k_6), and the rate constant of glucose leaving peritoneal cavity (k_a) because these rate constants were not significantly different between lean and obese mice based on our previous studies [20].

2.6. Statistical analysis

Results are expressed as mean ± SEM. Differences between means were evaluated using the Wilcoxon-Mann-Whitney test because the distribution of the data for some parameters were not normally distributed. Significant differences are indicated by *$p < 0.05$, **$p < 0.01$, and ***$p < 0.001$, respectively.

3. Results and discussion

Figure 1A shows weight gain of mice fed with lean diet or HFD over 28 weeks (7 months). Mice fed with HFD gained weight rapidly during the first 10 weeks, followed by steady increase over time. After 28 weeks of HFD feeding, weight gain of the mice was more than doubled (23.6 ± 0.5 g vs. 52.3 ± 1.4 g). Mice fed with lean diet showed a similar trend but at significantly lower levels at all the time points. Figure 1B and C shows fasting blood glucose levels of mice fed with lean diet- or HFD during the first 10 weeks. Fasting blood glucose levels of HFD-fed mice, showed

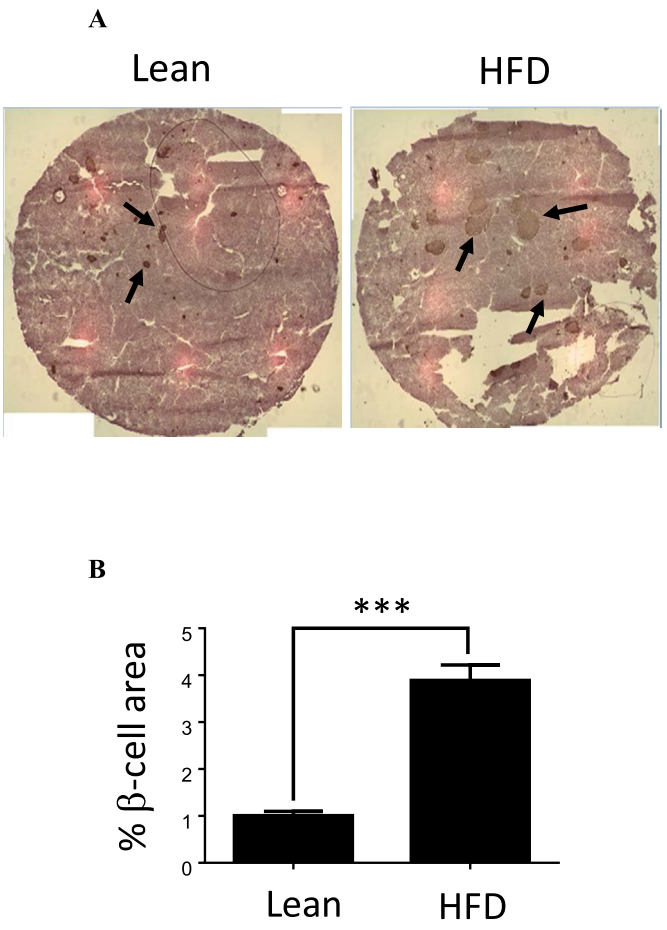

Figure 5. (A) Changes of % β-cell area in islets after 4 months of lean diet- or HFD-feeding. Frozen pancreas sections (10 μm) were treated with insulin rabbit mAb and biotinylated secondary antibody, followed by staining with AB enzyme reagent and peroxidase substrate containing DAB chromagen. Tissues were counterstained with hematoxylin. The figure shows representative images of pancreas sections. (B) The bar graph shows the ratio of β-cell area over exocrine tissue determined using the ImageJ image processing and analysis program. Data are the means ± SEM of pancreas sections of lean diet- (n = 12) and HFD-fed mice (n = 21) from 3 mice per condition.

significant intra- and inter-variability even during the first 10 weeks of HFD feeding (Figure 1C) and over time (Figure 2A and B). Fasting blood glucose and insulin levels of lean diet-fed mice, however, did not alter significantly despite weight gain or aging up to 2 years (Figure 1B and unpublished observations). Moreover, lean diet-fed mice showed normal glucose tolerance unaffected by weight gain or aging (unpublished observations). Therefore, we had not anticipated significant alterations in the parameters of glucose-insulin homeostasis in these mice. We have also previously compared 9 different parameters between lean- and HFD-fed mice after 3 months of the respective diets, which showed significant increases in basal insulin, k_3, and I_{pi} but significant decreases in k_2 and k_4 in HFD-fed mice as compared to lean diet-fed mice [17]. To minimize resource and effort, therefore, we tracked 8 HFD-fed mice for 28 weeks.

Presentation of all data for 8 mice on a graph was confusing and difficult to interpret due to peaks and troughs overlapping on top of each other. Therefore, we elected to present two representative data and a summary graph that contains baseline (0 week), average of 3 highest values (middle), and end (28^{th} week) during the course of obesity.

Figure 2A and B shows fasting blood glucose levels of two representative mice over time. The mice showed different patterns of peaks and troughs despite the same genetic background and the same diet, demonstrating inter-variability in the regulation of glucose-insulin homeostasis. The mean values of fasting blood glucose levels before and after the 28 weeks of HFD feeding were 152.8 ± 7.0 mg/dl and 152.0 ± 7.2 mg/dl, respectively, with the average of the three highest values of 216.8 ± 4.9 mg/dl (Table 1). The mice displayed elevated fasting blood glucose levels above 200 mg/dl for ~18 weeks (average) out of 28 weeks of HFD feeding. However, the elevated fasting blood glucose levels returned to the baseline at the end of 28 weeks in all of them (Figure 2C). As an extension of this study, we have monitored some of the HFD-fed mice close to 2 years of age with their body weights reaching ~70 g. Remarkably, none of them developed overt diabetes despite doubling of the body weights. Two potential reasons are proposed; 1) genetic predisposition for β-cell failure is not as strong in mice as in humans, and 2) relatively small mass of muscle in mice compared to humans leads to mild insulin resistance. In fact, compensatory responses including hypersecretion of insulin, pathologic alteration in the liver that reduces glucose release, and a significant increase in insulin-independent glucose uptake (k_3) seem to be sufficient to prevent development of overt diabetes.

Figure 3A and B shows changes of basal (fasting) blood insulin levels over time for two representative mice determined by radioimmunoassay. Basal insulin levels also showed fluctuations over time but they were significantly elevated at the end of the experimental period (Figure 3C) unlike fasting blood glucose levels. Insulin levels in the blood are primarily determined by insulin secretion and insulin clearance as shown in Eq. (2) of the mathematical model in the Methods section. In our previous study, the rate constant for insulin clearance was slightly elevated in HFD-fed mice as compared to lean diet-fed mice after three months of the respective diets although statistical significance was not reached [20]. The primary location of insulin clearance in the body is the liver [23]. About 80% of insulin released from pancreatic β-cells is extracted by the liver through endocytosis of insulin and insulin receptor complex, followed by degradation of insulin by insulin degrading enzyme (IDE) [24]. How insulin clearance and IDE expression and its activity alter in the setting of obesity, however, is controversial. Both elevation [25, 26] and reduction [27, 28] of these have been observed in diet-induced obesity animal models depending on the species. We postulate that β-cell mass expansion and reduction in insulin clearance are two independent compensatory responses to insulin resistance induced by obesity. The plasticity of β-cell expansion may affect the extent to which insulin clearance alters. In B6D2F1 mice we believe that the primary factor that contributes to basal insulin level is insulin secretion from pancreatic β-cells. As shown in Figure 4A and B, the rate constants for insulin secretion (k_1) of two representative mice showed similar rising patterns as basal insulin. As anticipated, both basal insulin and the rate constants of insulin secretion showed high peak values that occurred at different times for different mice, demonstrating inter-variability of the mice in the regulation of glucose-insulin homeostasis during the course of obesity. The primary compensatory response against insulin resistance is hypersecretion of insulin from pancreatic β-cells via expansion of β-cell mass and enhanced β-cell function [29, 30, 31].

Figure 5A shows remarkable increases in islet size (% β-cell area) in mice fed with HFD as compared to mice fed with lean diet after 4 months of the respective diets. Black arrows show individual islets embedded in the pancreatic exocrine tissues. The pancreases isolated from the HFD-fed mice were much more fragile than those from lean diet-fed mice due to ectopic lipid accumulation in the pancreas as shown in Figure 5A. In order to account for the loss of tissues due to breakage, the empty space within the pancreas sections was subtracted when the ratio of β-cell area per exocrine tissues was calculated and more samples were processed. Figure 5B shows the summary of % β-cell area obtained from lean (n = 12) and HFD-fed mice (n = 21). Increased islet size and number in HFD-

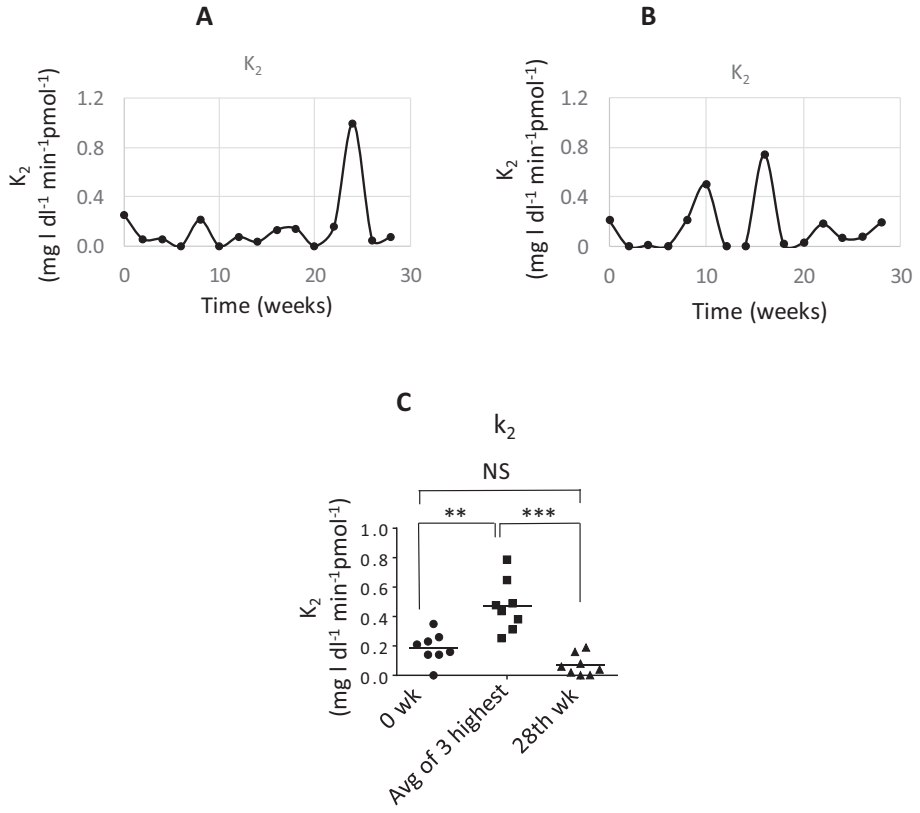

Figure 6. (A) and (B) Changes of the rate constant (k_2) of insulin-dependent glucose uptake of two representative mice over 28 weeks. (C) Mean values of k_2 (n = 8) at start (wk 0), during (average of 3 highest values), and end (wk 28) are shown.

fed mice have been extensively studied previously [32, 33, 34]. Moreover, HFD altered not only the architecture of islets but also percent α-cells [34]. Normal healthy rodent islets contain β-cells in the center and α-cells in the periphery of the islet [32, 33, 34]. HFD caused α-cells to migrate towards the center of the islet. Interestingly, % α-cells in islets from HFD-fed mice were significantly lower than those from lean diet-fed mice, suggesting that α-cells do not expand as readily as β-cells. We postulate that elevated basal insulin levels and the rate constants for insulin secretion (k_1) at the 28th week of HFD feeding contributed, in part, to maintaining fasting blood glucose levels within the normal range in these mice.

Figure 6A and B shows changes of insulin-dependent glucose uptake (k_2) over time for two representative mice. The fluctuations of k_2, especially elevated levels, were unexpected. In animals and humans, muscle mass expansion and enhanced insulin sensitivity with exercise may lead to an increase in k_2 [15,35,36]. The mice in cages, however, were not expected to have fluctuations in muscle mass or insulin sensitivity from week to week. With expansion of adipocytes due to HFD, muscle mass more likely decreased or remained the same in these mice. Therefore, we anticipated that insulin-dependent glucose uptake would decrease over time during the course of obesity as insulin resistance develops. We postulate that elevated levels of k_2 may reflect compensatory mechanisms of the body's attempt to sustain blood glucose levels within the normal range in the setting of obesity. It is a novel and new concept that compensatory responses to insulin resistance may occur not only in the insulin-secreting β-cells but also in the peripheral tissues such as muscle, liver, and adipocytes. Mechanisms of elevated k_2 may include increased glucose transporter synthesis and its translocation to the cell surface as well as higher V_{max} of glucose transporters despite impaired insulin receptor signaling. The cyclic pattern with peaks and troughs and eventual decrease of k_2 may represent the natural course of alterations in insulin-dependent glucose uptake during obesity. It is noteworthy that all 8 mice showed the similar low values of k_2 at the 28th week of HFD feeding (Figure 6C), suggesting that insulin resistance in the peripheral tissues ensue eventually despite compensatory increases of k_2 during the course of obesity. Similar to k_2, k_4 also showed cyclic pattern with peaks and troughs and eventual decrease at the end of the 28 weeks of HFD feeding (Figure 7), suggesting that glucose transfer in and out of the liver also fluctuated greatly in response to metabolic alterations during obesity. The similar changes of k_2 and k_4 support the impact of obesity on insulin-sensitive tissues as a whole. Although it is only at one time point (4 months after the respective diets), we have studied alterations in insulin signaling by examining the ratio of P-Akt/total Akt in the liver, heart, and skeletal muscle tissues isolated from lean- and HFD-fed mice injected with 0.65 U/kg insulin 5 min prior to asphyxiation by CO_2 [34]. All three tissues isolated from HFD-fed mice showed lower levels of p-Akt as compared to those from lean diet-fed mice [34], suggesting insulin resistance had developed in these tissues, corroborating low values of k_2 and k_4 found in the current study.

We have previously observed that the rate constants for insulin-independent glucose uptake into tissues (k_3) were much higher in the HFD-fed mice than those in the lean diet-fed mice after 3 months of HFD feeding [20]. Increased body mass of the HFD-fed mice and perhaps increased number of glucose transporters that transport glucose into tissues in an insulin-independent manner due to expanded fat pads, blood volume (increased blood cells), etc. were thought to be responsible for increased k_3. Figure 8A and B shows changes of k_3 over time in two representative HFD-fed mice. It is remarkable and interesting how k_3 fluctuates much more dynamically than other rate constants in these mice. Adipose tissue has been reported to account for only a small

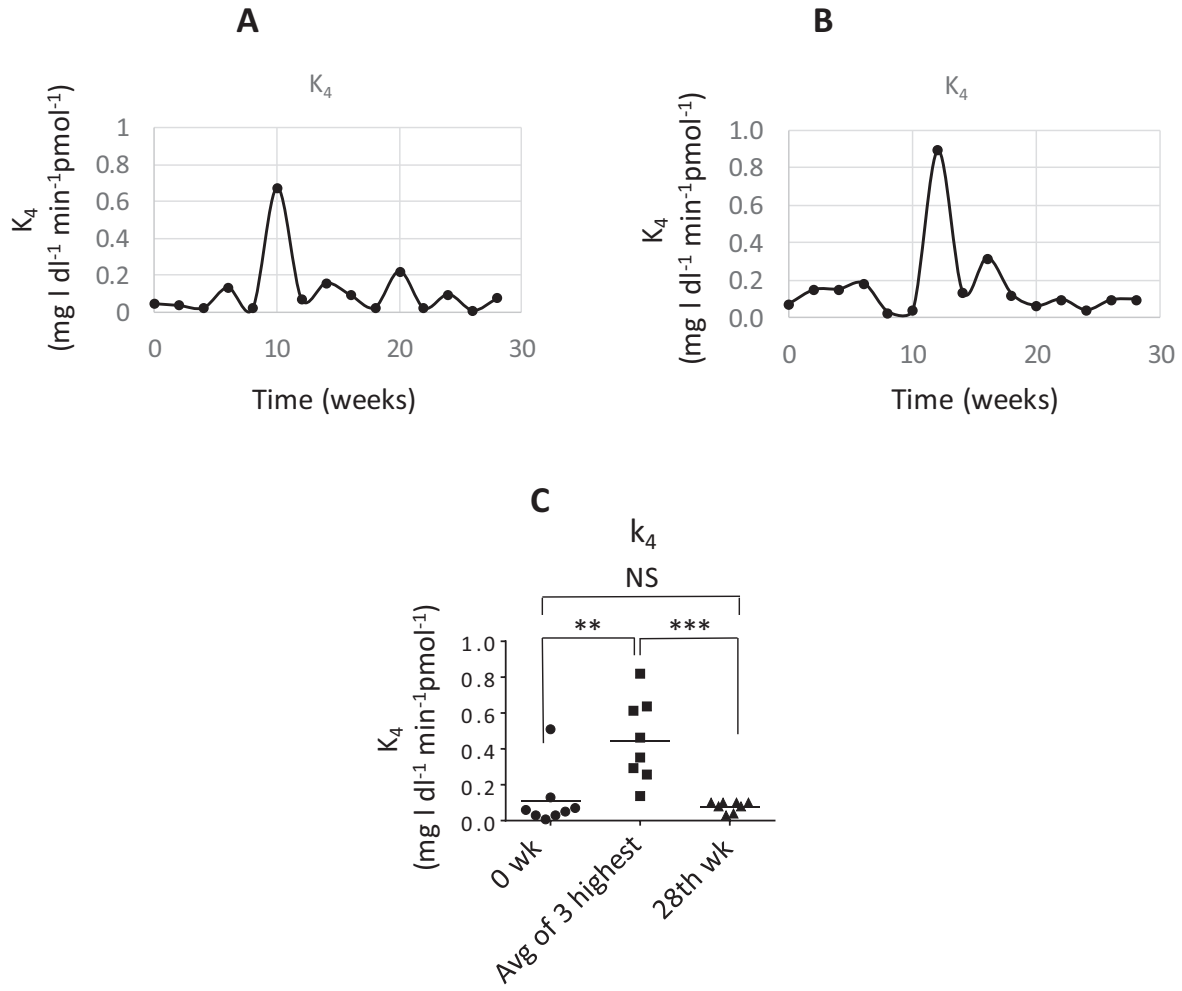

Figure 7. (A) and (B) Changes of the rate constant (k_4) of liver glucose transfer of two representative mice over 28 weeks. (C) Mean values of k_4 (n = 8) at start (wk 0), during (average of 3 highest values), and end (wk 28) are shown.

percentage (~7%) of total glucose uptake in animals and non-obese subjects [37, 38, 39]. However, in the setting of obesity, adipose tissue may play a significant role in glucose disposal via insulin-independent pathway. Evidence indicates that increased total fat mass in morbid obese individuals provides a sink for excess glucose and compensate for insulin resistance [40]. Interestingly, insulin-independent glucose uptake is thought to be responsible for as high as 70% of the whole body glucose disposal during fasting state [41] and the major determinants of glucose tolerance [42, 43]. The dynamic changes of k_3 over the course of obesity imply the plasticity of this rate constant and support the notion of exploring insulin-independent glucose uptake as potential targets for new therapies.

Figure 9A and B shows changes of insulin concentration where liver switches from glucose uptake to release (I_{pi}) over time for two representative mice. Similar to k_3, I_{pi} showed high-amplitude fluctuations, demonstrating the plasticity of this rate constant. The liver switch is sensitive to blood insulin levels. As basal insulin levels fluctuate during the course of obesity, I_{pi} seems to fluctuate as well to reset the liver switch as protective mechanisms. In these mice I_{pi} values after 7 months of HFD feeding were elevated similar to basal insulin levels but overall lower than blood insulin levels, favoring glucose uptake into the liver. This trend of liver handling of glucose and elevated insulin-independent glucose uptake (k_3) may be responsible for low fasting blood glucose levels in these mice.

4. Conclusions

In this paper, we studied the changes of metabolic states of the mice fed with lean diet or HFD. It is noteworthy how diet affects metabolic state of the mice much more significantly than weight gain per se or aging. Since lean diet-fed mice had not shown significant changes in fasting blood glucose levels or glucose tolerance, we tracked HFD-fed mice for 28 weeks and studied the alterations of fasting glucose and insulin levels along with 5 rate constants that determine glucose-insulin homeostasis. The key finding of the study is the wide range of fluctuations of virtually all rate constants over the course of obesity. It is natural for the body to show compensatory responses to the metabolic changes occurring due to obesity. However, it is unexpected that peripheral tissues in addition to pancreatic β-cells would show compensatory responses during the course of obesity. Enhancing the body's natural compensatory responses may be a potential therapeutic target. In fact, the mechanisms of actions of some of the oral hypoglycemic agents may involve boosting the body's compensatory responses in the peripheral tissues. Non-invasive yet accurate assessment of the rate constants of glucose-insulin homeostasis would be highly valuable in designing 1) customized drug therapy, targeting specific defect(s) of a patient, thus, delay the progression of the disease and its associated complications, and 2) customized individual algorithms for closed-loop artificial pancreas system in the future.

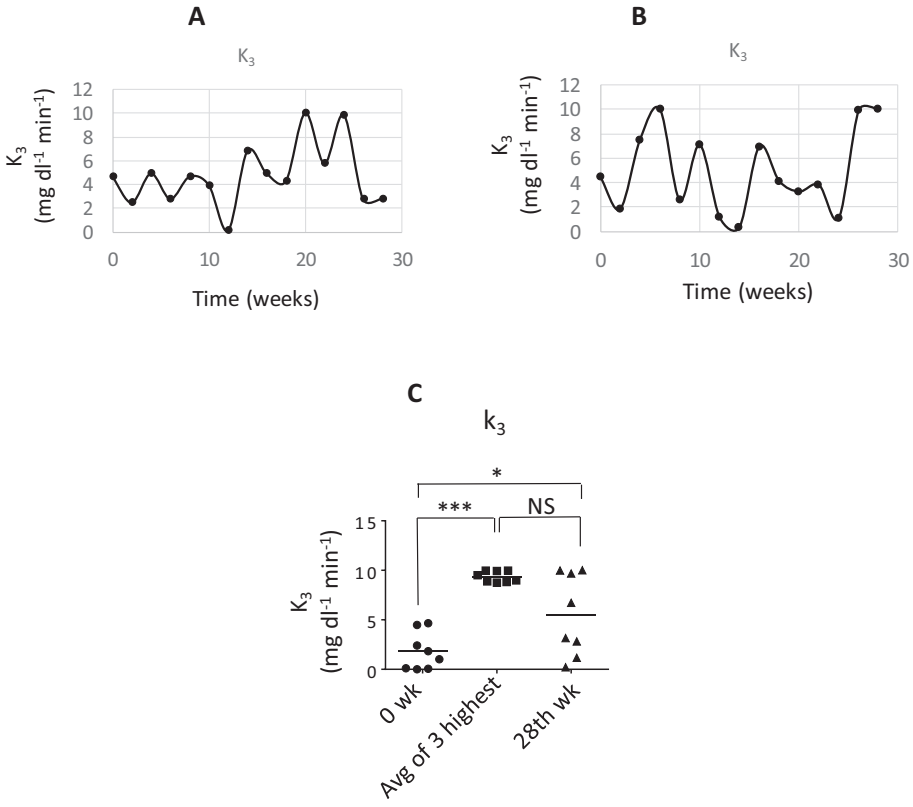

Figure 8. (A) and (B) Changes of the rate constant (k_3) of insulin-independent glucose uptake of two representative mice over 28 weeks. (C) Mean values of k_3 (n = 8) at start (wk 0), during (average of 3 highest values), and end (wk 28) are shown.

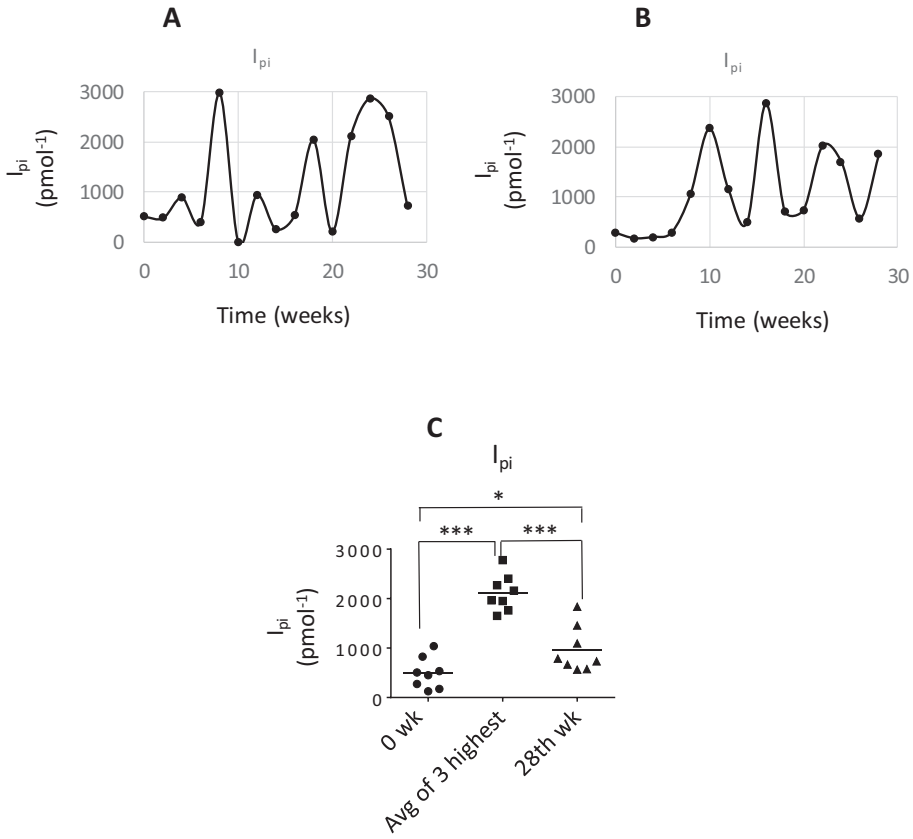

Figure 9. (A) and (B) Changes of the rate constant (I_{pi}) of insulin concentration where liver switches from glucose uptake to release of two representative mice over 28 weeks. (C) Mean values of I_{pi} (n = 8) at start (wk 0), during (average of 3 highest values), and end (wk 28) are shown.

Declarations

Author contribution statement

Sakineh Esmaeili Mohsen Abadi: Performed the experiments.

Ramin Balouchzadeh, Guney Uzun, Sarah Park: Analyzed and interpreted the data.

Hoo Sang Ko: Analyzed and interpreted the data; Wrote the paper.

H. Felix Lee: Conceived and designed the experiments; Analyzed and interpreted the data.

Guim Kwon: Conceived and designed the experiments; Analyzed and interpreted the data; Wrote the paper.

Funding statement

This work was support by SIUE Internal Grants.

Competing interest statement

The authors declare no conflict of interest.

Additional information

No additional information is available for this paper.

References

[1] J.M. Rytka, S. Wueest, E.J. Schoenle, D. Konrad, The portal theory supported by venous drainage-selective fat transplantation, Diabetes 60 (1) (2011) 56–63. Epub 2010/10/20. PubMed PMID: 20956499; PubMed Central PMCID: PMCPMC3012197.

[2] O.T. Hardy, R.A. Perugini, S.M. Nicoloro, K. Gallagher-Dorval, V. Puri, J. Straubhaar, et al., Body mass index-independent inflammation in omental adipose tissue associated with insulin resistance in morbid obesity, Surg. Obes. Relat. Dis. 7 (1) (2011) 60–67. Epub 2010/08/04. PubMed PMID: 20678967; PubMed Central PMCID: PMCPMC2980798.

[3] J. Kovsan, M. Bluher, T. Tarnovscki, N. Kloting, B. Kirshtein, L. Madar, et al., Altered autophagy in human adipose tissues in obesity, J. Clin. Endocrinol. Metab. 96 (2) (2011) E268–E277. Epub 2010/11/05. PubMed PMID: 21047928.

[4] S.E. Kahn, R.L. Prigeon, D.K. McCulloch, E.J. Boyko, R.N. Bergman, M.W. Schwartz, et al., Quantification of the relationship between insulin sensitivity and beta-cell function in human subjects. Evidence for a hyperbolic function, Diabetes 42 (11) (1993) 1663–1672. Epub 1993/11/01. PubMed PMID: 8405710.

[5] J.B. Meigs, P.W. Wilson, C.S. Fox, R.S. Vasan, D.M. Nathan, L.M. Sullivan, et al., Body mass index, metabolic syndrome, and risk of type 2 diabetes or cardiovascular disease, J. Clin. Endocrinol. Metab. 91 (8) (2006) 2906–2912. Epub 2006/06/01. PubMed PMID: 16735483.

[6] C.R. Kahn, D. Vicent, A. Doria, Genetics of non-insulin-dependent (type-II) diabetes mellitus, Annu. Rev. Med. 47 (1996) 509–531. Epub 1996/01/01. PubMed PMID: 8712800.

[7] G. Boden, Effects of free fatty acids (FFA) on glucose metabolism: significance for insulin resistance and type 2 diabetes, Exp. Clin. Endocrinol. Diabetes 111 (3) (2003) 121–124. PubMed PMID: 12784183.

[8] G. Pilon, A. Charbonneau, P.J. White, P. Dallaire, M. Perreault, S. Kapur, et al., Endotoxin mediated-iNOS induction causes insulin resistance via ONOO(-) induced tyrosine nitration of IRS-1 in skeletal muscle, PLoS One 5 (12) (2010), e15912. Epub 2011/01/06. PubMed PMID: 21206533; PubMed Central PMCID: PMC3011021.

[9] E. Bachar, Y. Ariav, M. Ketzinel-Gilad, E. Cerasi, N. Kaiser, G. Leibowitz, Glucose amplifies fatty acid-induced endoplasmic reticulum stress in pancreatic beta-cells via activation of mTORC1, PLoS One 4 (3) (2009), e4954. PubMed PMID: 19305497.

[10] U. Ozcan, Q. Cao, E. Yilmaz, A.H. Lee, N.N. Iwakoshi, E. Ozdelen, et al., Endoplasmic reticulum stress links obesity, insulin action, and type 2 diabetes, Science 306 (5695) (2004) 457–461. Epub 2004/10/16. PubMed PMID: 15486293.

[11] S.E. Kahn, The relative contributions of insulin resistance and beta-cell dysfunction to the pathophysiology of Type 2 diabetes, Diabetologia 46 (1) (2003) 3–19. Epub 2003/03/15. PubMed PMID: 12637977.

[12] B. Ahren, G. Pacini, Islet adaptation to insulin resistance: mechanisms and implications for intervention, Diabetes Obes. Metab. 7 (1) (2005) 2–8. Epub 2005/01/12. PubMed PMID: 15642070.

[13] R.A. DeFronzo, J.D. Tobin, R. Andres, Glucose clamp technique: a method for quantifying insulin secretion and resistance, Am. J. Physiol. 237 (3) (1979) E214–E223. Epub 1979/09/01. PubMed PMID: 382871.

[14] J.E. Ayala, D.P. Bracy, C. Malabanan, F.D. James, T. Ansari, P.T. Fueger, et al., Hyperinsulinemic-euglycemic clamps in conscious, unrestrained mice, J. Vis. Exp. 57 (2011). Epub 2011/12/01. PubMed PMID: 22126863; PubMed Central PMCID: PMCPMC3308587.

[15] M. Lombarte, M. Lupo, G. Campetelli, M. Basualdo, A. Rigalli, Mathematical model of glucose-insulin homeostasis in healthy rats, Math. Biosci. 245 (2) (2013) 269–277. Epub 2013/08/06. PubMed PMID: 23911696.

[16] H. Karasawa, S. Nagata-Goto, K. Takaishi, Y. Kumagae, A novel model of type 2 diabetes mellitus based on obesity induced by high-fat diet in BDF1 mice, Metab. Clin. Exp. 58 (3) (2009) 296–303. PubMed PMID: 19217442.

[17] A.C. Heijboer, E. Donga, P.J. Voshol, Z.C. Dang, L.M. Havekes, J.A. Romijn, et al., Sixteen hours of fasting differentially affects hepatic and muscle insulin sensitivity in mice, J. Lipid Res. 46 (3) (2005) 582–588. Epub 2004/12/04. PubMed PMID: 15576835.

[18] J.E. Ayala, D.P. Bracy, O.P. McGuinness, D.H. Wasserman, Considerations in the design of hyperinsulinemic-euglycemic clamps in the conscious mouse, Diabetes 55 (2) (2006) 390–397. Epub 2006/01/31. PubMed PMID: 16443772.

[19] H. Prior, L. Ewart, J. Bright, J.P. Valentin, Refinement of the charcoal meal study by reduction of the fasting period, Altern. Lab. Anim. 40 (2) (2012) 99–107. Epub 2012/07/06. PubMed PMID: 22762194.

[20] M. Brenner, S.E.M. Abadi, R. Balouchzadeh, H.F. Lee, H.S. Ko, M. Johns, et al., Estimation of insulin secretion, glucose uptake by tissues, and liver handling of glucose using a mathematical model of glucose-insulin homeostasis in lean and obese mice, Heliyon 3 (6) (2017), e00310. Epub 2017/06/20. PubMed PMID: 28626803; PubMed Central PMCID: PMCPMC5463011.

[21] F. Maher, T.M. Davies-Hill, P.G. Lysko, R.C. Henneberry, I.A. Simpson, Expression of two glucose transporters, GLUT1 and GLUT3, in cultured cerebellar neurons: evidence for neuron-specific expression of GLUT3, Mol. Cell. Neurosci. 2 (4) (1991) 351–360. Epub 1991/08/01. PubMed PMID: 19912819.

[22] I.A. Simpson, D. Dwyer, D. Malide, K.H. Moley, A. Travis, S.J. Vannucci, The facilitative glucose transporter GLUT3: 20 years of distinction, Am. J. Physiol. Endocrinol. Metab. 295 (2) (2008) E242–E253. Epub 2008/06/26. PubMed PMID: 18577699; PubMed Central PMCID: PMCPMC2519757.

[23] D.C. Polidori, R.N. Bergman, S.T. Chung, A.E. Sumner, Hepatic and extrahepatic insulin clearance are differentially regulated: results from a novel model-based analysis of intravenous glucose tolerance data, Diabetes 65 (6) (2016) 1556–1564. Epub 2016/03/20. PubMed PMID: 26993071; PubMed Central PMCID: PMCPMC4878413.

[24] W.C. Duckworth, R.G. Bennett, F.G. Hamel, Insulin degradation: progress and potential, Endocr. Rev. 19 (5) (1998) 608–624. Epub 1998/10/30. PubMed PMID: 9793760.

[25] X. Wei, B. Ke, Z. Zhao, X. Ye, Z. Gao, J. Ye, Regulation of insulin degrading enzyme activity by obesity-associated factors and pioglitazone in liver of diet-induced obese mice, PLoS One 9 (4) (2014), e95399. Epub 2014/04/18. PubMed PMID: 24740421; PubMed Central PMCID: PMCPMC3989328.

[26] A. Castell-Auvi, L. Cedo, V. Pallares, M. Blay, A. Ardevol, M. Pinent, The effects of a cafeteria diet on insulin production and clearance in rats, Br. J. Nutr. 108 (7) (2012) 1155–1162. Epub 2011/12/14. PubMed PMID: 22152054.

[27] S.P. Kim, M. Ellmerer, E.L. Kirkman, R.N. Bergman, Beta-cell "rest" accompanies reduced first-pass hepatic insulin extraction in the insulin-resistant, fat-fed canine model, Am. J. Physiol. Endocrinol. Metab. 292 (6) (2007) E1581–E1589. Epub 2007/02/08. PubMed PMID: 17284579.

[28] P. Brandimarti, J.M. Costa-Junior, S.M. Ferreira, A.O. Protzek, G.J. Santos, E.M. Carneiro, et al., Cafeteria diet inhibits insulin clearance by reduced insulin-degrading enzyme expression and mRNA splicing, J. Endocrinol. 219 (2) (2013) 173–182. Epub 2013/08/21. PubMed PMID: 23959080.

[29] T.L. Jetton, J. Lausier, K. LaRock, W.E. Trotman, B. Larmie, A. Habibovic, et al., Mechanisms of compensatory beta-cell growth in insulin-resistant rats: roles of Akt kinase, Diabetes 54 (8) (2005) 2294–2304. Epub 2005/07/28. PubMed PMID: 16046294.

[30] S.C. Hanley, E. Austin, B. Assouline-Thomas, J. Kapeluto, J. Blaichman, M. Moosavi, et al., {beta}-Cell mass dynamics and islet cell plasticity in human type 2 diabetes, Endocrinology 151 (4) (2010) 1462–1472. Epub 2010/02/24. PubMed PMID: 20176718.

[31] Y. Saisho, A.E. Butler, E. Manesso, D. Elashoff, R.A. Rizza, P.C. Butler, Beta-cell mass and turnover in humans: effects of obesity and aging, Diabetes Care 36 (1) (2013) 111–117. Epub 2012/08/10. PubMed PMID: 22875233; PubMed Central PMCID: PMCPMC3526241.

[32] S. Vernier, A. Chiu, J. Schober, T. Weber, P. Nguyen, M. Luer, et al., Beta-cell metabolic alterations under chronic nutrient overload in rat and human islets, Islets 4 (6) (2012) 379–392. Epub 2012/12/19. PubMed PMID: 23247575; PubMed Central PMCID: PMC3605166.

[33] M. Johns, R. Fyalka, J.A. Shea, W.L. Neumann, S. Rausaria, E.N. Msengi, et al., SR-135, a peroxynitrite decomposing catalyst, enhances beta-cell function and survival in B6D2F1 mice fed a high fat diet, Arch. Biochem. Biophys. 577–578 (2015) 49–59. Epub 2015/05/04. PubMed PMID: 25935364; PubMed Central PMCID: PMC4533897.

[34] M. Johns, S. Esmaeili Mohsen Abadi, N. Malik, J. Lee, W.L. Neumann, S. Rausaria, et al., Oral administration of SR-110, a peroxynitrite decomposing catalyst, enhances glucose homeostasis, insulin signaling, and islet architecture in B6D2F1 mice fed a high fat diet, Arch. Biochem. Biophys. 596 (2016) 126–137. Epub 2016/03/13. PubMed PMID: 26970045.

[35] E.A. Richter, L.P. Garetto, M.N. Goodman, N.B. Ruderman, Muscle glucose metabolism following exercise in the rat: increased sensitivity to insulin, J. Clin. Investig. 69 (4) (1982) 785–793. Epub 1982/04/01. PubMed PMID: 6804492; PubMed Central PMCID: PMCPMC370132.

[36] J.F. Wojtaszewski, B.F. Hansen, Gade, B. Kiens, J.F. Markuns, L.J. Goodyear, et al., Insulin signaling and insulin sensitivity after exercise in human skeletal muscle, Diabetes 49 (3) (2000) 325–331. Epub 2000/06/27. PubMed PMID: 10868952.

[37] K.N. Frayn, S.W. Coppack, S.M. Humphreys, P.L. Whyte, Metabolic characteristics of human adipose tissue in vivo, Clin. Sci. (Lond.) 76 (5) (1989) 509–516. Epub 1989/05/01. PubMed PMID: 2721118.

[38] P. Bjorntorp, P. Berchtold, J. Holm, B. Larsson, The glucose uptake of human adipose tissue in obesity, Eur. J. Clin. Investig. 1 (6) (1971) 480–485. Epub 1971/09/01. PubMed PMID: 5121738.

[39] S.W. Coppack, R.M. Fisher, S.M. Humphreys, M.L. Clark, J.J. Pointon, K.N. Frayn, Carbohydrate metabolism in insulin resistance: glucose uptake and lactate production by adipose and forearm tissues in vivo before and after a mixed meal, Clin. Sci. (Lond.) 90 (5) (1996) 409–415. Epub 1996/05/01. PubMed PMID: 8665779.

[40] P. Mitrou, E. Boutati, V. Lambadiari, E. Maratou, A. Papakonstantinou, V. Komesidou, et al., Rates of glucose uptake in adipose tissue and muscle in vivo after a mixed meal in women with morbid obesity, J. Clin. Endocrinol. Metab. 94 (8) (2009) 2958–2961. Epub 2009/05/14. PubMed PMID: 19435828.

[41] G. Pacini, K. Thomaseth, B. Ahren, Contribution to glucose tolerance of insulin-independent vs. insulin-dependent mechanisms in mice, Am. J. Physiol. Endocrinol. Metab. 281 (4) (2001) E693–703. Epub 2001/09/12. PubMed PMID: 11551845.

[42] J.D. Best, S.E. Kahn, M. Ader, R.M. Watanabe, T.C. Ni, R.N. Bergman, Role of glucose effectiveness in the determination of glucose tolerance, Diabetes Care 19 (9) (1996) 1018–1030. Epub 1996/09/01. PubMed PMID: 8875104.

[43] S.E. Kahn, R.L. Prigeon, D.K. McCulloch, E.J. Boyko, R.N. Bergman, M.W. Schwartz, et al., The contribution of insulin-dependent and insulin-independent glucose uptake to intravenous glucose tolerance in healthy human subjects, Diabetes 43 (4) (1994) 587–592. Epub 1994/04/01. PubMed PMID: 8138065.